Colloquium: Theory of quantum corrals and quantum mirages

Gregory A. Fiete*

Department of Physics, Harvard University, Cambridge, Massachusetts 02138, USA

Eric J. Heller[†]

*Department of Physics and Department of Chemistry and Chemical Biology,
Harvard University, Cambridge, Massachusetts 02138, USA*

(Published 16 July 2003)

Quantum corrals are two-dimensional structures built atom by atom on an atomically clean metallic surface using a scanning tunneling microscope (STM). These two-dimensional structures "corral" electrons in the surface states of noble metals, leading to standing-wave patterns in the electron density inside the quantum corral. The authors review the physics of quantum corrals and relate the signal of the STM to the scattering properties of substrate electrons from atomic impurities supported on the surface. The theory includes the effects of incoherent surface-state electron scattering at the impurities and quantitively describes nearly all of the current STM data on quantum corrals, including the recent quantum mirage experiments with Kondo effect. The physics underlying the recent mirage experiments is discussed, as are some of the outstanding questions regarding the Kondo effect from impurities in nanoscale structures on metallic surfaces. The authors also summarize recent work on variations of "quantum" corrals: Optical corrals and acoustical corrals.

CONTENTS

I. INTRODUCTION

Quantum corrals are the beautiful result of a marriage between technology and basic science. They are built atom by atom (using approximately 30–80 atoms) on atomically smooth metallic surfaces using a scanning tunneling microscope (STM).[1] Once the corrals are built, the STM (footnote 2) can be used to study these nanometer scale structures with atomic resolution in space and better than meV resolution in energy. The data of the STM can be rendered in false color to produce breathtaking images[3] that reveal standing-wave patterns of coherent electrons inside the corrals.

The history of quantum corrals begins with the pioneering work of Eigler and Schweizer (1990) who were the first to demonstrate that the STM could be used to controllably move atoms from place to place on the surface of a substrate. Not long afterwards, Crommie *et al.* (1993a) built the first quantum corrals from iron atoms on the Cu(111) surface and imaged standing-wave patterns inside them. In the early experiments it was thought that "stadium"-shaped corrals could be used as a laboratory to study "quantum chaos" (Heller *et al.*, 1994, 1995; Crommie *et al.*, 1995, 1996) but the walls proved too leaky (and the states of the corrals too low in energy) for the electrons to bounce around the (unstable) periodic orbits long enough to detect any "scarring" effects (Heller, 1984). A very intriguing recent STM corral experiment was done by Manoharan *et al.* (2000) who combined the physics of quantum corrals with the Kondo effect to achieve a beautiful "mirage" inside the corral of the spatially localized spectroscopic response of a Kondo impurity where there was in fact no Kondo impurity. The mirage experiment achieves this by taking advantage of both the locally modified electron density in the corral[4] and the scattering properties of a Kondo impurity.

---

*Electronic address: fiete@cmt.harvard.edu
[†]Electronic address: heller@physics.harvard.edu
[1]The developers of the STM, Gerd Binnig and Heinrich Rohrer, were awarded the Nobel Prize for Physics in 1986.

[2]For a more detailed discussion of the STM see Chen (1993).
[3]For a stunning demonstration of the sorts of images that can be produced with STM data see http://www.almaden.ibm.com/vis/stm/catalogue.html
[4]Kliewer, Berndt, and Crampin (2000) studied the effect of

In this Colloquium we review the scattering theory of STM measurements of quantum corrals including the recent mirage experiments with Kondo effect. We demonstrate the success of the scattering theory in reproducing *every* detail of the experiments including the electron standing-wave patterns, the energies and widths of corral states, and all features of the quantum mirage. The scattering theory we present is based on a single-particle picture but takes the many-body physics of the Kondo effect into account phenomenologically in a straightforward way. At the end of this Colloquium we discuss extensions of the quantum corrals to optical corrals and acoustical corrals. We begin our discussion with a review of the important physics of the substrate on which quantum corrals are built.

II. THE IMPORTANCE OF SURFACE STATES

The beautiful standing-wave patterns observed in STM corral experiments (Crommie *et al.*, 1993a; Heller *et al.*, 1994; Kliewer, Berndt, and Crampin, 2000; Manoharan *et al.*, 2000) result from the presence of Shockley surface states[5] on the metallic substrate. These are the same surface states responsible for the standing-wave patterns observed near a step edge (Hasegawa and Avouris, 1993). Surface states are the result of a particular crystallographic cut of the material, usually a noble metal, which places the Fermi energy in a band gap for electrons propagating normal to the surface. The surface states of Cu(111), Au(111), and Ag(111) are commonly used in STM experiments. In the direction normal to the surface (and in a range of angles around the normal), Bloch states are forbidden at the Fermi energy. However, solutions to the Schrödinger equation exist with exponentially decaying amplitude into both the bulk material and the vacuum. For such solutions electrons are still free to move in the plane of the surface and form a type of two-dimensional electron gas there. Often, the surface-state band is only partially filled, giving a low density on the surface, and a nearly quadratic dispersion relation with a constant effective mass.

The scattering theory that we develop for quantum corrals in Sec. IV is based on these free two-dimensional surface-state electrons. We will see that although the quantum corrals are two-dimensional systems in many respects, there are some important ways in which the underlying bulk material makes its presence felt. This is especially true with the quantum mirage experiments in

which the bulk electrons play an important role in the formation of the Kondo resonance (Knorr *et al.*, 2002).

Before we leave our brief discussion of surface states it is important to give some typical numerical values of important quantities such as the wavelength of electrons in the surface states, λ, the effective mass of surface-state electrons, m^*, and the density of states of the surface-state electrons, ϱ_{surf}. These three quantities are all related through the dispersion relation

$$E_{surf}(k) - E_F = E_0 + \frac{\hbar^2 k^2}{2m^*}, \tag{1}$$

where $\varrho_{surf} = m^*/\pi\hbar^2$ (for $E > E_0$) includes both spin-up and spin-down electrons. In the cases of Cu(111), Au(111), and Ag(111) the surface-state band minimum, E_0, is very close to the Fermi energy. Typical values are fractions of an eV below the Fermi energy (Kevan and Gaylord, 1987), E_F, where E_F is measured relative to the bottom of the bulk state bands and is typically 5–10 eV. For Cu(111), $E_0 \approx -450$ MeV and $m^* = 0.38 m_e$ with m_e the mass of the free electron. The surface-state electron density of Cu(111) is $n \approx 7 \times 10^{13}$ cm^{-2} which corresponds to approximately one surface-state electron per 12 Å$\times$12 Å square.

There are three important physical consequences of small E_0. The first is that it makes the dispersion relation quadratic and *isotropic* (in the plane of the surface) to a very good approximation. An isotropic dispersion relation is very convenient for the application of scattering theory because one does not need to know the orientation of the underlying crystal lattice. Second, a small E_0 makes the filling of the surface-state band rather low compared to bulk bands, which in turn makes the typical wavelength of the surface-state electrons, $\lambda \approx \lambda_F = 2\pi/k_F$, very large compared to the lattice spacing and the size of atomic impurities on the surface. For Cu(111), $\lambda_F = 29.5$ Å. Since λ_F is much larger than the underlying Cu(111) lattice spacing, the standing-wave patterns are easy to separate from atomic scale charge-density variations and since λ_F is large compared to the surface adatoms, we can make an *s*-wave approximation in the scattering theory.[6] Third, a small E_0 makes the electron filling small so the density of surface states is small compared to bulk states at the same energy. This has implications for the microscopic details of the Kondo effect from a magnetic impurity such as Co on the Cu(111) surface. We will return to this point in Sec. VIII. We now turn to the STM measurement.

---

the corral-modulated surface-state electron density on the spectroscopy of Mn on Ag(111), which did not display a Kondo effect.

[5]For more details see Davison and Steslicka (1996) and for experimental results for several materials see Kevan and Gaylord (1987). The surface states themselves are still a very active area of research with many STM studies being reported in recent years: Li, Schneider, Berndt, Bryant, and Crampin (1998a); Bürgi *et al.* (1999); Kliewer, Berndt, Chulkov, Silkin, Echenique, and Crampin (2000).

---

[6]The scattering theory we describe below is a two-dimensional theory. The dynamics in the direction normal to the surface is assumed to be energetically inaccessible, much like the case of a two-dimensional electron gas that forms at the interface of GaAs/AlGaAs. Electron scattering out of the plane of the surface (into the bulk) is taken into account in a phenomenological way in the scattering theory by adding an imaginary component to the phase shift. This is discussed in detail in Sec. IV.

Tunneling Geometry

(a)

STM Tip

ψ_t

Surface   d ψ_ν

Corresponding Energy Diagram

(b)

E_F^t

E_F^ν
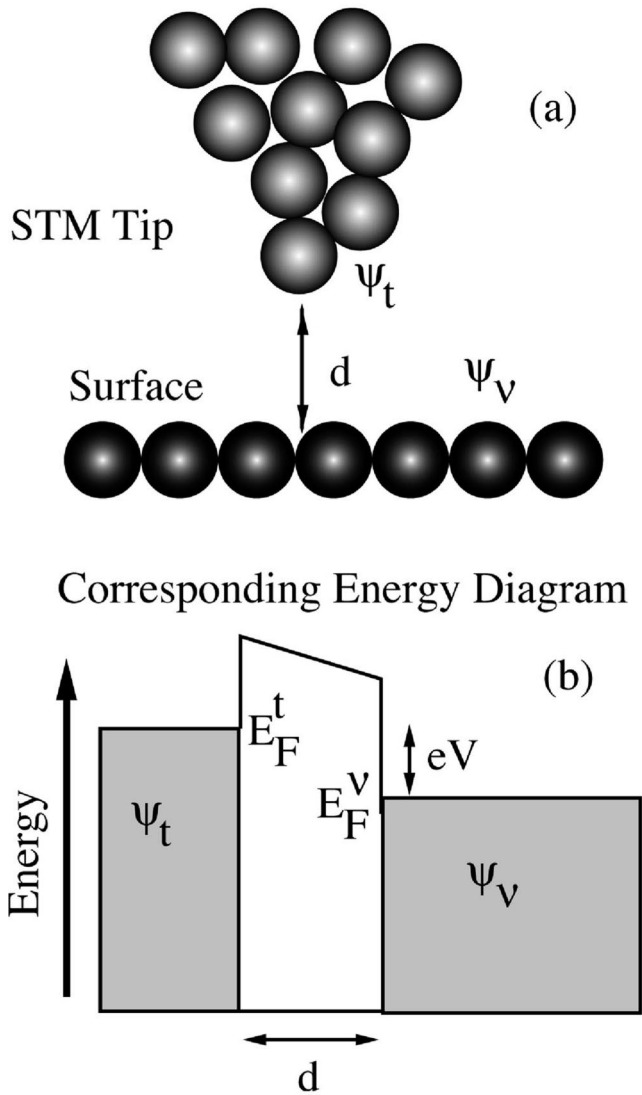
eV

ψ_t ψ_ν

Energy

d

FIG. 1. Geometry of the scanning tunneling microscope measurement and energy diagram. (a) Schematic of the STM tip above the substrate. The STM tip states are labeled ψ_t and the eigenstates of the substrate are labeled ψ_ν. The current is exponentially sensitive to the tip-surface distance, d. (b) Energy diagram of the tunneling process. Electrons must tunnel across a vacuum barrier of thickness d from occupied states of the tip to unoccupied states of the surface (energies $E_F^\nu < \epsilon < E_F^t$). The total current, Eq. (5), is given by the sum of all such processes, while the conductance, Eq. (6), just measures the tunneling rate for electrons at a particular energy in this window.

III. STM THEORY: TOPOGRAPHIC IMAGES AND SPECTROSCOPIC MEASUREMENT

In this section we briefly review the physics of the tunneling measurement. The basic tunneling geometry and energy diagram is shown in Fig. 1. The STM tip usually sits a few Å above the surface. The STM data can be taken in two ways: (i) A feedback loop can be

used to control the height of the tip above the surface so that the total tunneling current is kept constant as the tip is scanned over the surface. This is called a "topographic" image and, as we soon see, at each point it is a measure of the *energy-integrated* local density of surface states. (ii) In the second type of measurement the feedback loop is opened so that the tip height is kept roughly constant with respect to the surface and the voltage is swept to measure the local spectroscopy at the tip position.

Tunneling measurements of quantum corrals are typically done at small voltage biases, $V < 0.3$ V, and low temperatures, $T < 70$ K. In such a situation perturbation theory can be applied to compute the tunneling current in terms of the unperturbed tip states and surface states. According to Fermi's golden rule, the current at position **r** and STM bias voltage V is (Tersoff and Hamann, 1985; Bracher *et al.* 1997)

$$I(\mathbf{r}) = \frac{2\pi e}{\hbar} \sum_{t,\nu} |M_{t,\nu}(\mathbf{r})|^2 f(\epsilon_t)$$
$$\times [1 - f(\epsilon_\nu)] \delta(\epsilon_t + eV - \epsilon_\nu), \tag{2}$$

where e is the charge of the electron, t (ν) labels the tip (surface) states, f is the Fermi function, and $M_{t,\nu}(\mathbf{r})$ is the matrix element from the tip state t to the surface state ν at position **r**. The expression, Eq. (2), has a simple physical interpretation. It says that the tunneling current is proportional to the square of the matrix element connecting the various tip states to the various surface states times a factor which gives the probability of an occupied tip state and an empty surface state. The delta function enforces energy conservation. Finally all tip states and surface states are summed over. When the tip is treated as a point source, then $|M_{t,\nu}(\mathbf{r})|^2 \propto |\psi_\nu(\mathbf{r})|^2$ (Tersoff and Hamann, 1985), where $\psi_\nu(\mathbf{r})$ are the eigenfunctions of the surface. Assuming also that the temperature is low enough to replace the Fermi functions by step functions, using the relation $\int d\omega \, \delta(\epsilon_t + eV - \omega) \delta(\omega - \epsilon_\nu) = \delta(\epsilon_t + eV - \epsilon_\nu)$ and converting the sum over tip states to an integral, we obtain

$$I(\mathbf{r}) \propto \int_0^{eV} \varrho_t(\epsilon) \mathrm{LDOS}(\mathbf{r}, \epsilon) d\epsilon, \tag{3}$$

where $\varrho_t(\epsilon)$ is the density of states of the tip and the local density of states (LDOS) is given by

$$\mathrm{LDOS}(\mathbf{r}, \epsilon) = \sum_\nu |\psi_\nu(\mathbf{r})|^2 \delta(\epsilon - E_\nu). \tag{4}$$

Usually the density of states of the tip is assumed constant so that it can be pulled out of the integral,

$$I(\mathbf{r}) \propto \int_0^{eV} \mathrm{LDOS}(\mathbf{r}, \epsilon) d\epsilon, \tag{5}$$

and

$$\frac{dI}{dV}(\mathbf{r}, \epsilon) \propto \text{LDOS}(\mathbf{r}, \epsilon). \tag{6}$$

The last three equations above, Eqs. (4)–(6), are the most important formulas for the interpretation of the quantum corral experiments. The central quantity to calculate is Eq. (4) since the current, Eq. (5), and the conductance, Eq. (6), depend on it. The LDOS is expressed in terms of the eigenstates, labeled by ν, of the surface. It is through the calculation of these eigenstates from scattering theory that Eq. (4) provides the bridge between scattering theory and the tunneling measurement of the STM. We develop this connection fully in Sec. IV. From Eqs. (5) and (6) it is evident that the STM signal is related to the square of the surface-state wave functions at a given location. If the wave function has large (small) amplitude at a particular location, the current and conductance will tend to be larger (smaller) there.

A topographic measurement corresponds to Eq. (5) in which a feedback loop is used to modulate the tip height to keep the current constant. This is usually the type of measurement used to produce data such as the standing-wave patterns in quantum corrals. Typical bias voltages are on the order of 10 meV so that the current at position $\mathbf{r}$ is an integral over approximately 10 meV of energy. In most experiments, the density of states at any given position $\mathbf{r}$ does not vary much over 10 meV. However, in the mirage experiments the Kondo effect actually produces strong variations in the local density of states over 10 meV (Manoharan *et al.*, 2000)

In the spectroscopic measurement the STM tip-surface distance is held fixed by turning off the feedback loop. The voltage is swept (at a given position) to reveal the energy dependence of the LDOS, Eq. (6). This is the type of measurement that reveals the energies and widths of resonances in quantum corrals which appear as peaks in a plot of dI/dV vs V. The Kondo resonance at a Kondo impurity also has a strong signature in dI/dV (Li, Schneider, Berndt, and Delley, 1998; Madhavan *et al.*, 1998; Manoharan *et al.*, 2000). The quantum mirage is most easily probed in this way (Manoharan *et al.*, 2000; Fiete *et al.*, 2001).

IV. SCATTERING THEORY FOR SURFACE-STATE ELECTRON DENSITY

In this section we develop a scattering theory for the electron density in quantum corrals. In Sec. II we emphasized the importance of the surfaces states on the (111) surfaces of noble metals and gave the important properties for the development of scattering theory: two-dimensional electron states on the surface, isotropic and parabolic dispersion of the energy, and long electron wavelength compared to the lattice spacing and the size of the adatoms. We now describe the way in which the quantities of the STM measurement given in Sec. III, namely, Eq. (4), are obtained from scattering theory. The physical picture to have in mind is of a circularly symmetric electron amplitude emanating from the STM

tip into the surface states of the substrate.[7] This amplitude spreads radially outward from the tip until it encounters a defect (such as an impurity) on the surface or a step edge, at which time it scatters. Part of this amplitude is reflected back to the STM tip[8] (possibly scattering several more times along the way from different impurities) and interferes with the outgoing amplitude leading to fluctuations in the LDOS, and hence the tunneling current, as a function of position. Note that the fluctuations are a result of the *coherent* part of the backscattered amplitude.

Let the Hamiltonian of an electron on the surface be $\hat{H} = \hat{H}_0 + \hat{V}$, where $\hat{H}_0$ is the Hamiltonian describing free propagation in the surface states and $\hat{V}$ accounts for the spatially local and separate potential perturbations due to the impurities on the surface. The amplitude to propagate from point $\mathbf{r}$ to point $\mathbf{r}'$ in time t on the surface is given by the retarded Green's function, $G^{\text{ret}}(\mathbf{r}', \mathbf{r}, t) = -i\theta(t)\langle \mathbf{r}' | e^{-i\hat{H}t/\hbar} | \mathbf{r} \rangle$, where $\theta(t)$ is the step function. The eigenstates of $\hat{H}$ are the scattering eigenstates of the particle in the presence of the potential $\hat{V}$. Inserting a complete set of eigenstates,

$$G^{\text{ret}}(\mathbf{r}', \mathbf{r}, t) = -i\theta(t)\sum_\nu \langle \mathbf{r}' | e^{-iE_\nu t/\hbar} | \psi_\nu \rangle \langle \psi_\nu | \mathbf{r} \rangle, \tag{7}$$

and taking the Fourier transform of this,

$$G^{\text{ret}}(\mathbf{r}', \mathbf{r}, \epsilon) = \sum_\nu \frac{\psi_\nu^*(\mathbf{r})\psi_\nu(\mathbf{r}')}{\epsilon - E_\nu + i\delta}. \tag{8}$$

Here $\psi_\nu(\mathbf{r})$ are the eigenstates of the Hamiltonian $\hat{H}$ and δ is an infinitesimal positive quantity. For the STM measurements, we are interested in the part of the amplitude that backscatters to the tip. Thus, we are interested in $\mathbf{r}' = \mathbf{r}$. The imaginary part of the diagonal amplitude is proportional to the local density of states,

$$\text{LDOS}(\mathbf{r}, \epsilon) \equiv -\frac{1}{\pi}\text{Im}[G^{\text{ret}}(\mathbf{r}, \mathbf{r}, \epsilon)]$$

$$= \sum_\nu |\psi_\nu(\mathbf{r})|^2 \delta(\epsilon - E_\nu). \tag{9}$$

What we have established is a relationship between the full Green's function, Eq. (8), the scattering eigenstates of the Hamiltonian $\hat{H}$, $\psi_\nu(\mathbf{r})$, and the local density of states. What remains is to develop a method for calculating the Green's function, Eq. (8).

---

[7]By measuring the change in the differential conductance when the voltage is swept from below surface-state band energies to above the lowest surface-state band energy, the relative fraction of flux into the surface states and bulk states can be determined. It is typically around 50% (Bürgi *et al.*, 1998; Knorr *et al.*, 2002).

[8]The exponential decay of the surface states into the vacuum can affect the details of the topographic measurements due to the feedback loop (Kliewer *et al.*, 2001).
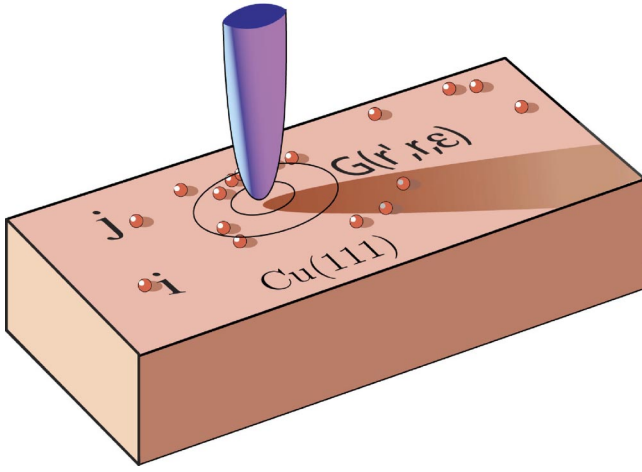
FIG. 2. (Color in online edition) Schematic of the scattering geometry of multiple-scattering theory. The scattering centers, shown as little beads, are adatoms on the surface of a noble metal such as Cu(111). In the approximation that the STM tip is pointlike, a circularly symmetric electron amplitude, $G_0(\mathbf{r}',\mathbf{r},\epsilon)$, emanates from the tip into the surface states of the metal and encounters the impurities on the surface. Since the wavelength of the electrons in the surface states is much larger than the size of the scatterers, one can treat the scatterers as s-wave scatterers and ignore all higher orbital channels. Because the scatterers are far apart compared to their size, we assume that electrons propagate freely between impurities. i and j label different impurities.

We first consider the case in which $\hat{V}$ represents a single scatterer. Dyson's equation can be written

$$\hat{G}^{\text{ret}}=\hat{G}_0^{\text{ret}}+\hat{G}_0^{\text{ret}}\hat{V}\hat{G}^{\text{ret}}, \tag{10}$$

where $\hat{G}^{\text{ret}}$ is the full retarded Green's function and $\hat{G}_0^{\text{ret}}$ is the free retarded Green's function. When $\hat{V}=0$, $\hat{G}^{\text{ret}}=\hat{G}_0^{\text{ret}}$. The $\hat{G}^{\text{ret}}$ on the right-hand side of Eq. (10) can be formally eliminated by iterating the equation. In operator notation,

$$\hat{G}^{\text{ret}}=\hat{G}_0^{\text{ret}}+\hat{G}_0^{\text{ret}}\hat{V}\hat{G}_0^{\text{ret}}+\hat{G}_0^{\text{ret}}\hat{V}\hat{G}_0^{\text{ret}}\hat{V}\hat{G}_0^{\text{ret}}+\cdots$$

$$=\hat{G}_0^{\text{ret}}+\hat{G}_0^{\text{ret}}(\hat{V}+\hat{V}\hat{G}_0^{\text{ret}}\hat{V}+\cdots)\hat{G}_0^{\text{ret}}. \tag{11}$$

The terms in the series have the physical interpretation of a particle that (i) does not scatter at all from the potential, (ii) scatters once and leaves, (iii) scatters once, propagates, scatters again, and then leaves, and so on to infinite order. Truncation of the series at $\hat{V}$, for example, is just the first Born approximation. The terms within parentheses can be grouped into a single object called the t matrix. The t matrix is defined by

$$\hat{T}=\hat{V}+\hat{V}\hat{G}_0^{\text{ret}}\hat{V}+\cdots. \tag{12}$$

When the spatial extent of the scattering potential is small compared to the wavelength of the incoming particle, as is the case for adatoms on the Cu(111) surface, the scattering is s wave (isotropic) because the wavelength of the incident particle is too large to "feel" the spatial structure of the target. In the s-wave approxima-

tion, the t matrix takes a particularly simple form in position representation (Rodberg and Thaler, 1967):

$$G^{\text{ret}}(\mathbf{r},\mathbf{r})=G_0^{\text{ret}}(\mathbf{r},\mathbf{r})+\int\int d^2\mathbf{r}'d^2\mathbf{r}''G_0^{\text{ret}}(\mathbf{r},\mathbf{r}')$$

$$\times s\,\delta(\mathbf{r}_0-\mathbf{r}'')\,\delta(\mathbf{r}_0-\mathbf{r}')G_0^{\text{ret}}(\mathbf{r}'',\mathbf{r}), \tag{13}$$

where $s(k)=(4i\hbar^2/m^*)[e^{2i\delta(\epsilon)}-1]$, $\mathbf{r}_0$ is the position of the impurity, and $\delta(\epsilon)$ is the energy-dependent phase shift $[\epsilon(k)$ is given by Eq. (1)] in the s-wave orbital channel [which can be computed once $V(r)$ is known or determined directly from experiment]. The integral can then be done trivially to yield

$$G^{\text{ret}}(\mathbf{r},\mathbf{r})=G_0^{\text{ret}}(\mathbf{r},\mathbf{r})+s\,G_0^{\text{ret}}(\mathbf{r},\mathbf{r}_0)G_0^{\text{ret}}(\mathbf{r}_0,\mathbf{r}). \tag{14}$$

Note that when $V(r)$ goes to zero, $\delta(\epsilon)$ goes to zero and one obtains $G^{\text{ret}}(\mathbf{r},\mathbf{r})=G_0^{\text{ret}}(\mathbf{r},\mathbf{r})$. That is, the full Green's function reduces to the free Green's function.

The extension to several scatterers is straightforward. The schematic situation is shown in Fig. 2. The new ingredient in the many-scatterer case is an extra self-consistency condition on the scattered amplitude. Imposing this self-consistency condition is equivalent to calculating the scattering among all the impurities to infinite order. This is the heart of multiple-scattering theory. (The t matrix gives the result of scattering from a single impurity to infinite order.)

In the presence of N scatterers the t-matrix equation $\Sigma_{i=1}^N\hat{T}_i\hat{G}_i^{\text{ret}}=\Sigma_{i=1}^N\hat{V}_i\hat{G}^{\text{ret}}$ ($\hat{V}_i$ are nonoverlapping scattering potentials and the $\hat{T}_i$ are the corresponding t matrices for these potentials) generalizes Eq. (13) to

$$G^{\text{ret}}(\mathbf{r},\mathbf{r})=G_0^{\text{ret}}(\mathbf{r},\mathbf{r})+\sum_{i=1}^N\int\int d^2\mathbf{r}'d^2\mathbf{r}''G_0^{\text{ret}}(\mathbf{r},\mathbf{r}')$$

$$\times s_i\delta(\mathbf{r}_i-\mathbf{r}'')\,\delta(\mathbf{r}_i-\mathbf{r}')G_i^{\text{ret}}(\mathbf{r}'',\mathbf{r})$$

$$=G_0^{\text{ret}}(\mathbf{r},\mathbf{r})+\sum_{i=1}^N s_iG_0^{\text{ret}}(\mathbf{r},\mathbf{r}_i)G_i^{\text{ret}}(\mathbf{r}_i,\mathbf{r}), \tag{15}$$

where the G_i^{ret} are the self-consistently calculated values of the Green's functions at the locations of the scatterers,

$$G_i^{\text{ret}}(\mathbf{r}_i,\mathbf{r})=G_0^{\text{ret}}(\mathbf{r}_i,\mathbf{r})+\sum_{j\neq i}^N s_iG_0^{\text{ret}}(\mathbf{r}_i,\mathbf{r}_j)G_j^{\text{ret}}(\mathbf{r}_j,\mathbf{r}), \tag{16}$$

and

$$s_i(\epsilon)=\frac{4i\hbar^2}{m^*}[e^{2i\delta_i(\epsilon)}-1], \tag{17}$$

for the ith scatterer. The solution of Eq. (16) is given by the equation

$$\mathbf{G}=\mathbf{A}^{-1}\mathbf{G_0}, \tag{18}$$

where $\mathbf{A}$ is an $N\times N$ matrix with elements $\mathbf{A}_{ij}=\delta_{ij}-s_iG_0(\mathbf{r}_i,\mathbf{r}_j)$, containing all the information about the propagation between the impurities, and $\mathbf{G_0}$ and $\mathbf{G}$ are N-dimensional column vectors of elements $\mathbf{G_{0i}}=G_0(\mathbf{r}_i,\mathbf{r})$ and $\mathbf{G}_i=G(\mathbf{r}_i,\mathbf{r})$, respectively, containing the

information about propagation from the STM tip to the impurities and from the impurities to the STM tip.

The STM signal is then calculated from scattering theory by specifying the s-wave scattering phase shifts $\delta_i(\epsilon)$, the locations $\{\mathbf{r}_i\}$ of the N impurities on the surface, and the incident electron amplitude. Given the dispersion relation, Eq. (1), the free Green's function, $G_0^{\text{ret}}(\mathbf{r}',\mathbf{r},\epsilon)$, is determined from Eq. (8) in the case of $\hat{V}=0$. In two dimensions, the outgoing Green's function from a point source is $G_0^{\text{ret}}(\mathbf{r}',\mathbf{r},\epsilon)=-i(m^*/2\hbar^2)[J_0(k|\mathbf{r}'-\mathbf{r}|)+iY_0(k|\mathbf{r}'-\mathbf{r}|)]$, where J_0 (Y_0) is the Bessel function of the first (second) kind. The final step is to fix the energy and then solve the system of equations, Eqs. (15) and (16), by means of Eq. (18) at the particular chosen energy. (All three of these equations depend on the energy and must be resolved for each new energy.) The solution is then substituted into Eq. (9), which directly gives the STM signal through Eqs. (5) and (6).

The theory just developed applies equally well to electrons or holes near the Fermi energy. Although the STM tip is the source (or sink in the case of positive bias, i.e., the tip has larger voltage) of electrons (or holes), we have not included one correction that, in principle, is present, namely, any residual unscreened potential felt by an electron near the STM tip. In fact the tip itself can be thought of as a source of scattering, causing disturbances to any electron passing under it. However, we have so far not seen any experimental evidence indicating this correction is needed at small bias voltages.[9]

V. APPLICATION TO QUANTUM CORRALS

The scattering theory of Sec. IV may be directly applied to quantum corrals. Here we discuss the case of Fe atoms on Cu(111) (Heller *et al.*, 1994) which do not show a Kondo effect at 4 K. Our goal is to calculate the standing-wave patterns and corral spectroscopy of the type first observed by Crommie *et al.* (1993a). To do so we pull together the results of Secs. II–IV. Since we know the dispersion relation, Eq. (1), for the Cu(111) surface as well as the positions of the iron impurities from STM measurements, all that remains to determine the current and conductance at a given position is a determination of the phase shift, $\delta(\epsilon)$, of the Fe atoms. Once $\delta(\epsilon)$ is determined, the LDOS$(\mathbf{r},\epsilon)$ is determined everywhere by the scattering theory except within 7 Å of an adatom, where there is extra charge density not accounted for in the theory. Electron amplitude from the STM tip is assumed to emanate in a circularly symmetric fashion into the surface states, so we use the outgoing free Green's function, $G_0^{\text{ret}}(\mathbf{r}',\mathbf{r},\epsilon)=-i(m^*/2\hbar^2)[J_0(k|\mathbf{r}'-\mathbf{r}|)+iY_0(k|\mathbf{r}'-\mathbf{r}|)]$, as the incident amplitude.

---

[9]At larger biases, there may be some Stark shifting of the states due to the electric field of the STM tip: There are differences in the surface-state band-edge energies for STM and photoemission experiments.
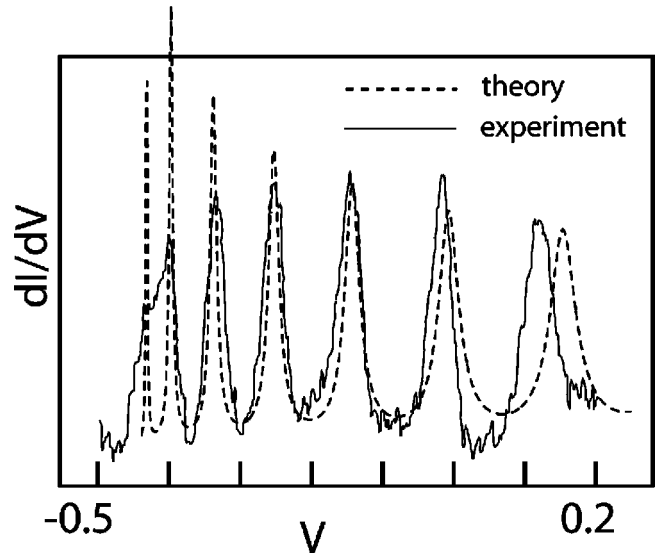

FIG. 3. The experimental and theoretical voltage dependence of dI/dV, with the tip of the STM located at the center of an 88.7-Å-radius, 60-atom circular corral of Fe atoms on a Cu(111) surface. A smooth background has been removed from the experimental data.

Early measurements (Crommie *et al.*, 1993b) of single iron impurities on the surface of Cu(111) pointed to a phase shift near $-80°$. However, from Eq. (17), it is clear that the Green's function is invariant with respect to a phase shift of π, so the phase shift could equally well have been near $+100°$. When the scattering theory was applied with a phase shift of $+100°$ to circular corrals to compute dI/dV, Eq. (6), the widths of the resonances were far too narrow compared to experiment, indicating a longer electron confinement than was actually inferred from the broader, measured linewidths. The important insight (Heller *et al.*, 1994) was that the resonances could be broadened if one allows electron amplitude to be absorbed from the surface states at the Fe impurities. A phase shift of nearly $+100°$ is quite close to $+90°$. This leads to

$$s_i(\epsilon)=\frac{4i\hbar^2}{m^*}[e^{2i\delta_i(\epsilon)}-1] \xrightarrow{\delta=\pi/2} \frac{4i\hbar^2}{m^*}(-2). \qquad (19)$$

On the other hand, if the Fe atoms were assumed to be maximally absorbing "black dots" (Heller *et al.*, 1994) $\delta=i\infty$, then

$$s_i(\epsilon)=\frac{4i\hbar^2}{m^*}[e^{2i\delta_i(\epsilon)}-1] \xrightarrow{\delta=i\infty} \frac{4i\hbar^2}{m^*}(-1), \qquad (20)$$

so that the overall scattering amplitude has the same phase but is reduced by a factor of 2. Thus, the two phase shifts, $\delta=\pi/2$ and $\delta=i\infty$, are equivalent except that the "black dot" approximation, $\delta=i\infty$, leads to an attenuation of the scattered wave and a broadening of corral resonance widths. When $\delta=i\infty$ is used to evaluate the LDOS$(\mathbf{r},\epsilon)$, at the center of a circular quantum corral, the agreement with experiment is excellent. Figure 3 shows a direct comparison between theoretical and experimental dI/dV curves for an 88.7-Å-radius, 60-atom

60 Fe Atom Circle On Cu(111)
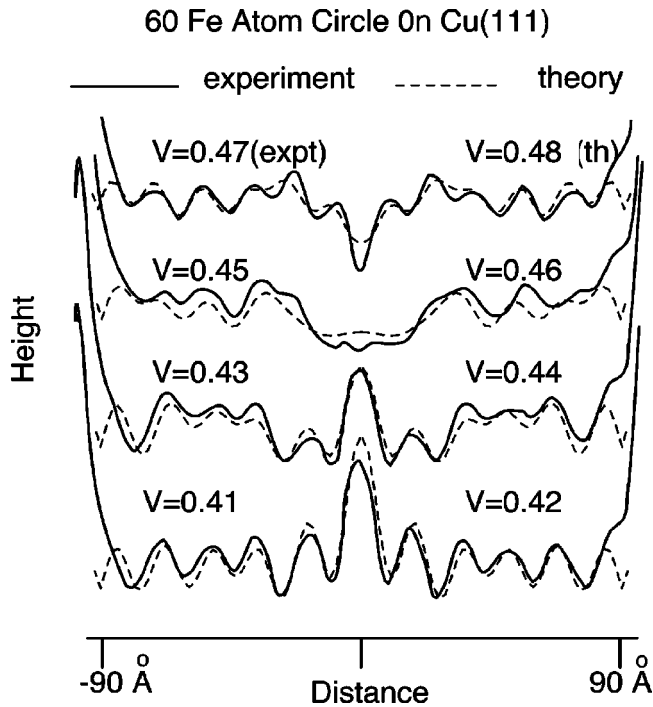
——— experiment - - - - - - - theory

FIG. 4. The experimental data and theoretical curves for the tip height as a function of position across the diameter of a circular corral (88.7 Å radius, 60 atoms) for low bias voltages. Various voltages are given (in volts, V); they are measured relative to the bottom of the surface-state band. Note that all theory voltage values are shifted by 0.01 V relative to experiment.

circular corral of Fe atoms on a Cu(111) surface. Note that except for the first peak[10] the agreement with experiment is excellent. Both the resonance energies and the widths of the resonances are remarkably alike and scale together except for the highest-energy peak.[11] Figure 4 shows a comparison between theory and experiment for a "topographic" image for a cut across the diameter of the same circular corral. Note again the excellent agreement: Every experimental oscillation is quantitatively reproduced by the scattering theory. Finally, the full standing-wave patterns for both theory and experiment for a "stadium"-shaped quantum corral are shown in Fig. 5.

The Fe adatoms can be located only at the available triangular lattice sites in the Cu(111) surface. This lattice allows arcs, ellipses, and other shapes to be only approximated. The locations at which one can place atoms can be seen in Fig. 6, for the case of a 48-atom stadium, where the smooth boundary is drawn for comparison. It is important to use the correct atomic positions for the best agreement with the experiments. The corral walls,

_____

[10]The first peak has been investigated in more detail by Crampin and Bryant (1996).

[11]The scattering theory can be brought into nearly perfect agreement with even the highest-energy peak by allowing for a quartic correction to the parabolic dispersion, Eq. (1) (Chan, 1997).
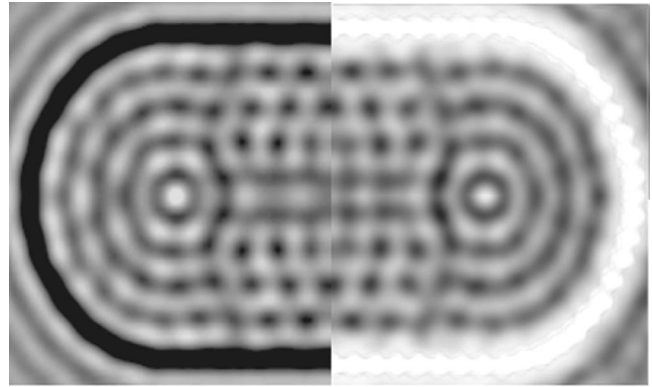

FIG. 5. Local density of electron states (LDOS) near E_F for a 76-Fe-atom "stadium" of dimensions 141×285 Å. Right-hand side: experiment, bias voltage 0.01 V ($\epsilon = 0.45$ eV); left-hand side: theory ($\epsilon = 0.46$ eV). The density at the locations of the Fe adatoms is not accounted for in the theory and appears black.

while acting like smooth (although absorbing) boundaries for some purposes, still reveal their roughness and granularity.

We now turn to a physical interpretation of the "black dot" approximation. If electron flux is absorbed at the Fe atoms where does it go? We believe that much of the lost surface-state amplitude goes into the bulk.[12] This idea has been supported by theoretical studies of Crampin *et al.* (1994) and Hormandinger and Pendry (1994). Shortly after the work of Heller *et al.* (1994), Harbury and Porod (1996) developed an elastic-scattering theory of quantum corrals. The elastic theory is able to qualitatively reproduce the standing-wave patterns inside the corrals but does relatively poorly compared to the inelastic-scattering theory for dI/dV. [See Fig. 3 in Harbury and Porod (1996).] The inelastic-scattering theory presented here accounts well (at energies higher than the first one or two peaks) for the widths and heights of the resonances in corrals compared to the elastic theory of Harbury and Porod (1996). However, at lower energies there is disagreement due to the intrinsic lifetime of the surface states that saturates the linewidths (Crampin and Bryant, 1996). This effect can be exploited in quantum corrals and near step edges to study many-body effects in the surface states (Crampin and Bryant, 1996). We return to this point in Sec. IX.

It is important to summarize what we have learned from the application of scattering theory to quantum corrals thus far: (i) Corrals do confine electrons in surface states, but do so rather poorly (resonance widths are broad) because the adatoms tend to couple surface states quite strongly to bulk states. A host of studies (Crampin *et al.*, 1994; Hormandinger and Pendry, 1994; Bürgi *et al.*, 1998; Fiete *et al.*, 2001; Knorr *et al.*, 2002; Schneider *et al.*, 2002) suggest that it is quite generic for

_____

[12]Spin-flip processes at the Fe impurities would also appear as a loss of coherent amplitude.
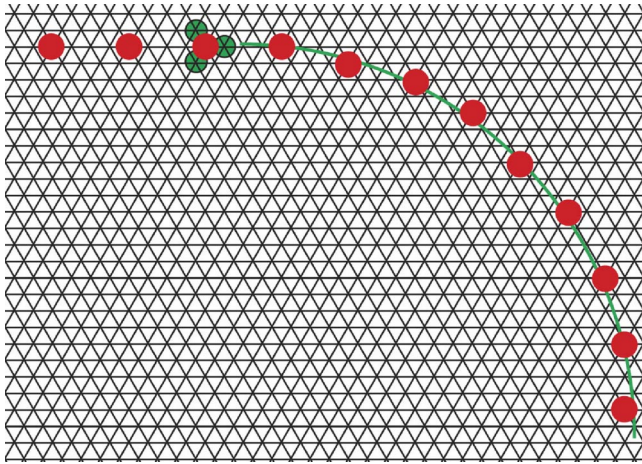
FIG. 6. (Color in online edition) Shown is a grid of the underlying lattice of the Cu(111) surface. Adatoms cannot sit at exact positions of an ideal stadium, ellipse, or circular-shaped corral, but must sit on the nearest site of the underlying lattice. When the exact positioning of the adatoms is taken into account in the theoretical calculations, the agreement with experiment is enhanced. At one site, four dark circles are shown. The lighter circles represent possible positions for the darker, central adatom. Obviously the central position is best for the geometry given by the solid line shown.

FIG. 7. A theoretical calculation of STM data that could not be modeled with a "particle-in-the-box" approximation (because it is "open") or any type of smooth arc (note the circular "wavelets" near the impurities).

adatoms to strongly couple surface states to bulk states. (ii) The standing-wave patterns in corrals depend on coherent electron propagation in the surface states to give interference effects. For temperatures below 70 K, the coherence length of surface-state electrons on noble metals is hundreds of angstroms (Jeandupeux *et al.*, 1999), while the corrals typically have maximum dimensions on the order of a hundred angstroms thus allowing coherent electron propagation across the corrals. (iii) "Particle-in-a-box" models (Crommie *et al.*, 1993a) may qualitatively agree with the observed resonance energies of closed structures, but they have no predictive power for resonance widths or standing-wave patterns in open structures. For example, consider the arc in Fig. 7; it shows predicted STM data with a variety of features that certainly could not be modeled with a box, or even, for some of the features, with a smooth arc imposing some boundary condition. Scattering theory works equally well for one atom as for any arbitrary arrangement of any number of atoms (provided the structure is small enough to allow coherent electron propagation across it). (iv) The only place the scattering theory fails to agree with experiment is within 7 Å of an atom. Here the assumptions of the theory break down because the extra charge density at the impurity is not properly accounted for.

One comment is in order on the multiple-scattering theory. As simple as it is to invert a matrix of the dimension equaling the total number of atoms to obtain the Green's function, it is still perhaps curious to do a multiple-scattering expansion in terms of $0,1,2,\ldots$ scattering events. It turns out that this fails for typical configurations, due to the presence of closely spaced pairs, triplets, etc., of atoms. Even though the Q factor of the
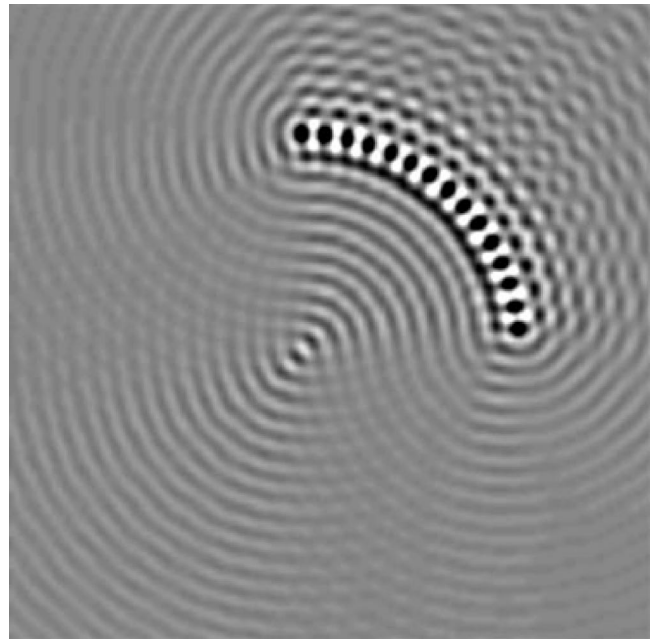
cavity, as indicated, for example, by the linewidths of the dI/dV resonances, is only around 2, suggesting that about two bounces are important before leakage occurs, the Q factor and the low order of scattering is an appropriate concept only for walls perceived as smooth scattering units, with the local multiple internal scattering between neighboring atoms included to infinite order.

The scattering theory does not have to confine itself only to atomic surface impurities. The experiments abound with step edges (Bürgi *et al.*, 1998, 1999; Jeandupeux *et al.*, 1999; Morgenstern *et al.*, 2002), for example, even though one looks for regions as far away as possible from such defects to build corrals. The step edges affect the images, although not so much inside closed corrals, which have enough attenuation at the wall to prevent those paths that begin inside the corral, get out, hit an edge, and come back inside, preventing them from having any important weight.

VI. THE MIRAGE EXPERIMENT

A recent and interesting variation of the original quantum corral experiments were the "quantum mirage" experiments[13] of Manoharan *et al.* (2000). The quantum mirage experiments make use of the low-temperature physics associated with a magnetic ion (e.g., Fe, Co, Mn) in electrical contact with a bulk metal (e.g., Cu, Au, Ag): the so-called Kondo effect. In the quantum

---

[13]For a more detailed description of the experiments we recommend that readers consult the original paper, Manoharan *et al.* (2000).
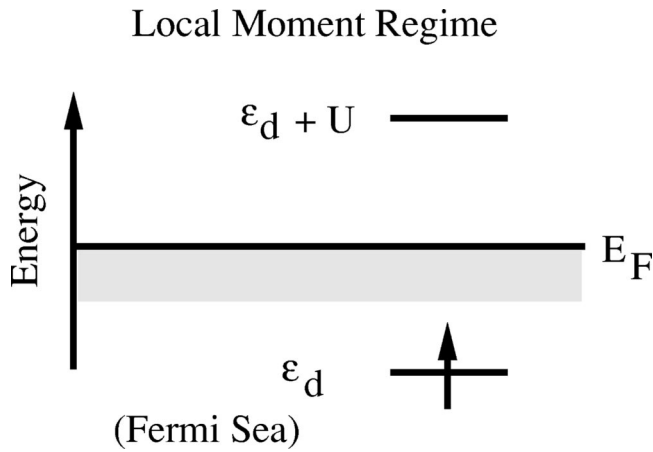
Local Moment Regime

FIG. 8. Local-moment regime of the Anderson model. The Kondo effect occurs when the impurity level energies are situated as shown. The spin degenerate singly occupied level has energy $\epsilon_d < E_F$. The cost for adding the second electron of opposite spin to the impurity level is $\epsilon_d + U > E_F$. Thus, the impurity ground state has only one electron on the local level, giving it a net spin.

mirage experiments, Manoharan *et al.* (2000) built an elliptical corral with magnetic atoms (Co) which exhibit a Kondo effect at 4 K on Cu(111).

The Kondo effect is the many-body response of the free electrons in the Fermi sea to the magnetic impurity; it is intimately related to spin-flip scattering events of free conduction electrons from the magnetic ion. To understand the problem in detail takes a substantial investment of time, but fortunately the results of a detailed analysis relevant to the quantum mirage can be stated quite simply and succinctly: (i) The spin of the conduction electrons tend to become anticorrelated (oppositely aligned) with the spin of the magnetic impurity so that at low temperatures (when the Kondo effect is present) the local spin of the magnetic ion is fully or at least partially screened. An important case occurs when the spin of the ion is 1/2. Then, the Kondo effect *completely* screens it at sufficiently large distances.[14] In the scattering approach that we are using, this means that spin-flip scattering is "frozen out" and we can treat the scattering as purely *potential scattering* (i.e., we neglect spin-flip scattering processes). We discuss in Sec. VII how this "freezing out" of the spin might be understood. (ii) The impurity density of states (the density of states of the atomic d or f levels that give rise to the magnetic moment) develops a narrow resonance near the Fermi energy that is often termed the "Kondo resonance." This resonance is picked up in the STM measurement and is the main spectroscopic signature of Kondo atoms.

The narrow Kondo resonance [whose width is related to the Kondo energy scale, $T_K \sim 50$ K for Co on

---

[14]Larger spins can also be completely screened, but require more than one orbital channel of the conduction electrons to couple to them. See Nozieres and Blandin (1980) for a discussion.
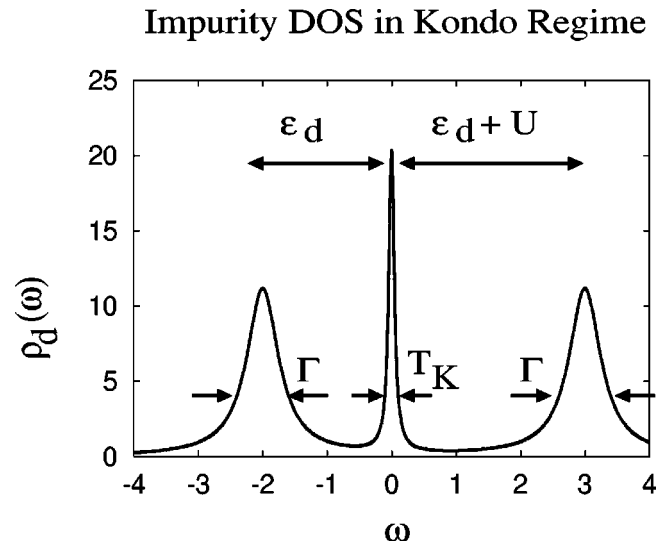
Impurity DOS in Kondo Regime

FIG. 9. Density of states of the Anderson impurity model in the Kondo regime. The figure is not an actual calculation but illustrates the central features of the density of states in the Kondo regime. Both axes are in arbitrary units, but for a real system energy units of eV would not be unrealistic. The broad upper and lower peaks (at energies ϵ_d and $\epsilon_d + U$) have width $\Gamma \approx 2\pi V^2 \varrho_0$. These peaks are due to single-particle energy levels of the impurity. They are broadened by coupling to the Fermi sea. The central peak is a many-body resonance sometimes called the "Kondo peak." It arises from correlations beyond a mean-field calculation such as Hartree Fock, and its width is exponentially small in the coupling parameter $J\varrho_0$, $T_K \sim D e^{-1/2J\varrho_0}$.

Cu(111)] appears in dI/dV near a Kondo atom. It had been observed near (within 10 Å) isolated atoms (Li, Schneider, Berndt, and Delley, 1998b; Madhavan *et al.*, 1998) earlier, but Manoharan *et al.* (2000) used the modification of the surface-state electron density in an elliptical quantum corral to produce a spectroscopic "mirage" inside the corral of a Kondo atom where there was in fact no Kondo atom (the "source" of the mirage was a Co atom inside the corral more than 70 Å away).[15] In order to fully understand the mirage experiment, we must first review some details and essential results of the theory of the Kondo effect. We will need these results for the application of our scattering theory to adatoms which show a Kondo effect.

VII. ESSENTIALS OF KONDO PHYSICS

A. The Anderson model

The Kondo effect[16] is the name given to the low-energy response of the Fermi sea of a metal to a mag-

---

[15]The experimental and theoretical spectroscopic signature is shown in Fig. 13 below.

[16]For an overview of Kondo effect and a list of references see Hewson (1997). For a brief survey of the Kondo effect in *mesoscopics* see Ujsághy *et al.* (2001), and references therein.

netic impurity. In the mirage experiments, the magnetic impurity (Co) sat on the surface of Cu(111). The canonical (and simplest) model[17] of a local magnetic moment in a metallic host was given by Anderson (1961),

$$\hat{H}_{\text{Anderson}} = \sum_{k,\sigma} \epsilon_{k\sigma} \hat{n}_{k\sigma} + \sum_{\sigma} \epsilon_d \hat{n}_{d\sigma} + U \hat{n}_{d\uparrow} \hat{n}_{d\downarrow}$$

$$+ \sum_{k,\sigma} (V \hat{c}_{k\sigma}^{\dagger} \hat{d}_{\sigma} + \text{H.c.}). \tag{21}$$

The first term represents the energy of the electrons of the Fermi sea (assumed to be noninteracting), the second term represents the energy of a single localized site (an approximation to the d or f atomic level of an atom), the third term represents an on-site repulsion if two electrons try to occupy the localized level, and the last term represents hybridization between the local moment and the conduction electrons. Here $\epsilon_{k\sigma}$ ($\hat{n}_{k\sigma}$) is the energy (number operator) of an electron of the Fermi sea with wave vector k and spin σ, and ϵ_d ($\hat{n}_{d\sigma}$) is the spin degenerate energy (number operator, not generally spin degenerate) of an electron in the localized d or f level with spin σ. Here U represents the charging energy of doubly occupying the localized level. In the fourth term, V is the hopping matrix element connecting the electrons of the Fermi sea to the localized impurity level and vice versa, and $\hat{c}_{k\sigma}^{\dagger}$ ($\hat{d}_{\sigma}^{\dagger}$) is the creation operator for an electron in the state with wave vector k (d or f level) with spin σ.

In the case $V=0$, Eq. (21) can be solved exactly. The states are just direct products of the local-moment states and the Fermi sea. The energy is just the sum of the energy of the Fermi sea and the energy of the electron(s) on the localized level. The energy cost for having one electron on the localized level is ϵ_d and the cost for adding the second is $\epsilon_d + U$. If one considers a small nonzero V, the Hamiltonian is no longer exactly solvable. The singly and doubly occupied states of the local level will be broadened (by an amount that can be estimated by Fermi's golden rule, $\Gamma \approx 2\pi V^2 \varrho_0$, where ϱ_0 is the density of states of the Fermi sea at the Fermi energy, or more precisely, at the energy ϵ_d, if the density of states varies with energy). For the Kondo problem one particular regime of Eq. (21) is of central importance: the case in which $\epsilon_d < E_F$ and $\epsilon_d + U > E_F$. This is shown in Fig. 8. Anderson (1961) showed that Eq. (21) will lead to local-moment formation at low enough temperatures when $\Gamma \approx 2\pi V^2 \varrho_0 \ll |\epsilon_d|,\ \epsilon_d + U$.

The impurity (d-level) density of states in the Anderson model in the local-moment regime we have just discussed is shown in Fig. 9. The peak in the density of states at zero bias is sometimes referred to as the

"Kondo" peak (Hewson, 1997). The Kondo peak always sits near the Fermi energy and corresponds to the formation of the *many-body* Kondo state. It is this peak that shows up in the form of a "Fano resonance" in the dI/dV spectra near (within 10 Å) a Kondo atom on the surface of a metal (Li, Schneider, Berndt, and Delley, 1998; Madhavan *et al.*, 1998; Manoharan *et al.*, 2000; Schiller and Hershfield, 2000; Újsághy *et al.*, 2000; Plihal and Gadzuk, 2001). Although the Kondo resonance is associated with many-body correlations of the Fermi sea and has no single-particle level analogous to the two spectral peaks corresponding to the bare levels at ϵ_d and $\epsilon_d + U$ in Fig. 9, it still *behaves* as a single-particle resonance when it is fully formed at $T \ll T_K$ (Nozieres, 1974; Újsághy *et al.*, 2000; Plihal and Gadzuk, 2001). It is this single-particle-like behavior or "local Fermi-liquid theory" (Nozieres, 1974) of the Kondo resonance that allows us to use a single-particle scattering theory for the mirage experiments. The density of states of Fig. 9 translates into a strongly energy-dependent phase shift for electrons of the Fermi sea near the Fermi energy (Hewson, 1997). For a single impurity in a host (or on the surface) the density of states is (to a good approximation) just the sum of the two: $\varrho(\epsilon) = \varrho_0(\epsilon) + \varrho_{\text{imp}}(\epsilon)$. Therefore, the change in the density of states due to the impurity is $\Delta\varrho(\epsilon) \equiv \varrho(\epsilon) - \varrho_0(\epsilon) = \varrho_{\text{imp}}(\epsilon)$. It can be shown to equal (Hewson, 1997),

$$\varrho_{\text{imp}}(\epsilon) = \frac{1}{\pi} \frac{\partial \delta(\epsilon)}{\partial \epsilon}. \tag{22}$$

The resonance at the Fermi energy in Fig. 9, for $\varrho_{\text{imp}}(\epsilon)$, can be approximated as a Lorentzian of width Γ centered near the Fermi energy (ϵ_0) and leads to a $\tan^{-1}[(\epsilon - \epsilon_0)/(\Gamma/2)]$ term in the phase shift $\delta(\epsilon)$ [cf. Eq. (27)] when Eq. (22) is integrated over energy. It is highly nontrivial that one can treat a many-body problem such as the Kondo effect phenomenologically with a single-particle theory and a resonant phase shift. It is the single most important reason for the success of our approach to the quantum mirage.

B. The Kondo model

The Kondo model is a special limit of the Anderson model, Eq. (21), valid in the local-moment regime shown in Fig. 8. It was used by Kondo (1964) (hence the name) to explain the minimum in the resistivity (as a function of temperature) of metals with magnetic impurities. The Kondo model can be derived by second-order perturbation theory in V from the Anderson model.[18] The Kondo Hamiltonian (including a purely potential scattering term that also appears in second-order perturbation theory) is

---

[17]The Anderson model applies to a spin $S=1/2$ impurity. However, it can be shown (Újsághy *et al.*, 2000) that impurities of higher spin can be treated with an effective spin $S=1/2$ model. For a discussion of the Kondo effect for spin $S > 1/2$ see Nozieres and Blandin (1980).

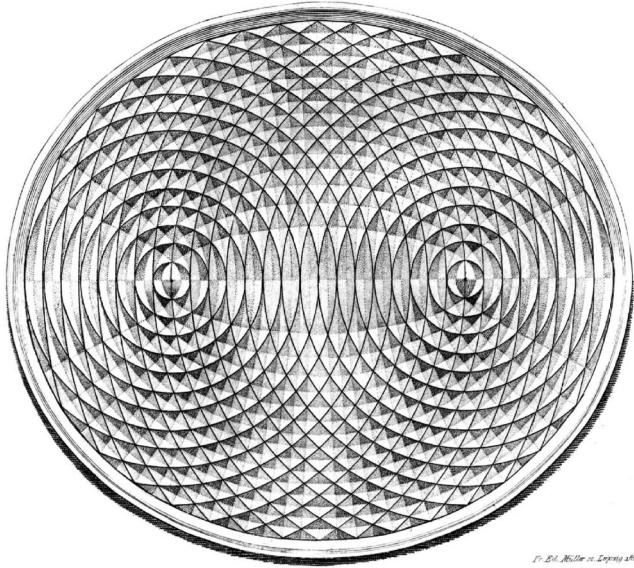[18]This result was first derived by Schrieffer and Wolf (1966).

FIG. 10. A sketch from *Wellenlehre* (*Wave Theory*), an 1825 book published in Leipzig by two of the three Weber brothers/ scientists from Saxony, Ernst and Wilhelm, showing the wave pattern of mercury waves when small amounts of mercury are dropped in at one focus. Notice how the other, opposite focus looks identical, indicating that from the point of view of the wave, the two foci are excited equally.

$$\hat{H}_{\text{Kondo}} = \sum_{k,\sigma} \epsilon_{k\sigma} \hat{n}_{k\sigma} + J \sum_{k,k'} \hat{S} \cdot \hat{c}_{k\sigma}^{\dagger} \frac{\vec{\tau}_{\sigma\sigma'}}{2} \hat{c}_{k'\sigma'}$$

$$+ K \sum_{k,k',\sigma} \hat{c}_{k\sigma}^{\dagger} \hat{c}_{k'\sigma}, \tag{23}$$

where the first term is the same as in Eq. (21),

$$J \approx V^2 \left(\frac{1}{U + \epsilon_d} - \frac{1}{\epsilon_d} \right) > 0, \tag{24}$$

and

$$K \approx -\frac{V^2}{2} \left(\frac{1}{U + \epsilon_d} + \frac{1}{\epsilon_d} \right). \tag{25}$$

Here $\hat{S}$ is the spin operator of the impurity and $\vec{\tau}$ are the Pauli spin matrices. The crucial feature of Eq. (23) is that it leads to spin-flip scattering events[19] through terms such as $S_x\tau_x + S_y\tau_y = (S_+\tau_- + S_-\tau_+)/2$. These terms turn out to be related to the apparent low-temperature divergence of the resistivity (as a function of temperature) in some metals with a low concentration of magnetic impurities (which are able to flip the spins of electrons). Kondo's explanation of the divergence is a result of looking at the effect of the second term of Eq. (23) in a second-

order perturbative calculation of the t matrix. It turns out that because $S_+S_- \neq S_-S_+$, one of the sums over the intermediate states of the Fermi sea is cut off at the Fermi surface, leading to a logarithmic divergence in the resistivity (Kondo, 1964; Hewson, 1997).

Besides the features of the Kondo problem we have already mentioned, one more result is worthy of note. In order to understand the low-energy behavior of many physical systems it is often useful to integrate out the high-energy fluctuations and compensate for this by "renormalizing" the parameters of an effective low-energy theory. This can be quite complicated in general, but for the Kondo Hamiltonian a particularly simple version known as "poor man's scaling," introduced by Anderson (1970), can be used to identify the low-energy properties (Hewson, 1997). The idea is to look again at the second-order contributions to the t matrix from the second term of Eq. (23). The sum over the intermediate states of the conduction electrons contains electrons that are at the band edges. Anderson suggested removing a few states at the band edges and adjusting J so that the scattering amplitude remains invariant (ignoring the potential scattering terms). When this is done a set of "scaling equations" is generated for J which can then be solved. It turns out that a "scaling invariant" appears and it is generally denoted by T_K and referred to as the Kondo temperature:

$$T_K = D e^{-1/2J\varrho_0}. \tag{26}$$

The quantity T_K is invariant under a rescaling of J in response to a shrinking of the bandwidth, D. As $D \rightarrow 0$, $J \rightarrow \infty$, which from the second term of Eq. (23) implies that the spin-flip processes are "frozen out" in the low-energy theory and the scattering becomes purely potential scattering. As before, ϱ_0 is the density of states of the host at the Fermi energy. The Kondo effect, in this simplest of models, is thus characterized by only one energy scale, T_K. This is the width of the "Kondo peak" that appears in the low-temperature density of states of the Anderson model in Fig. 9, the width of the Fano resonance (Li, Schneider, Berndt, and Delley, 1998; Madhavan *et al.*, 1998; Kawasaka *et al.*, 1999; Manoharan *et al.*, 2000; Schiller and Hershfield, 2000; Újsághy *et al.*, 2000; Plihal and Gadzuk, 2001), and the width of the scattering resonance (Fiete *et al.*, 2001), from Eq. (22), of the Co atoms on the surface of Cu(111) (for experimental temperatures lower than T_K when the Kondo resonance is well formed).

VIII. THEORY OF QUANTUM MIRAGES

In their fascinating quantum mirage experiment, Manoharan *et al.* (2000) decided to use the unique scattering properties of an ellipse in an attempt to project the properties of an atom sitting at one focus of the ellipse to the corresponding second (empty) focus of the ellipse. The ellipse has been recognized for its properties in the context of waves for a long time. For example, the remarkable image showing surface waves of mercury in an elliptical container (Fig. 10), drawn by two of the

---

[19]These spin-flip scattering events can also be looked at from the point of view of the Anderson model. A spin flip would occur if, e.g., the initial electron on the local level were spin up, a second spin-down electron hopped on in the intermediate state, and then finally the original spin-up electron hopped off, leaving behind the spin-down electron on the local level.
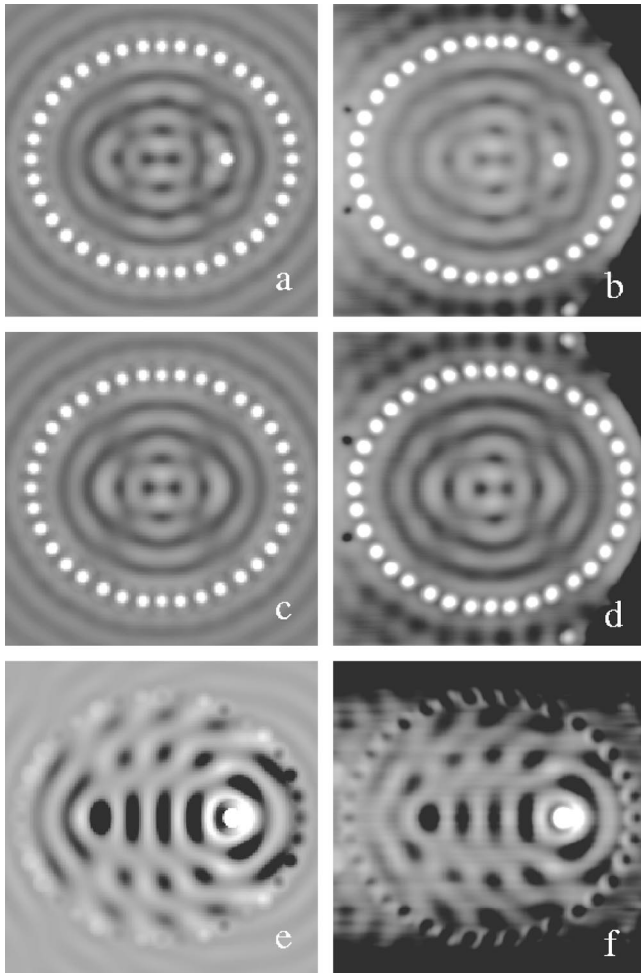
FIG. 11. Topographical standing-wave patterns of a Kondo corral. Using the scattering theory and phase shifts described in the text, these STM topographic images were computed using exact Co adatom positions on Cu(111) at 4 K. The agreement between theory (a), (c), and (e) and experiment (b), (d), and (f) is remarkable. All the experimental images have been symmetrized by adding the image to itself after being reflected about its major axis. Topographic images were calculated by numerically integrating the LDOS$(\vec{r},\epsilon)$ over ϵ for $E_F \lesssim \epsilon \lesssim E_F + 10$ mV. This corresponds to the topographic images taken experimentally in (b) and (d) at a bias voltage of 10 mV. (e) The difference of (a) and (c). (f) The difference of (b) and (d).

three scientifically inclined Weber brothers in 1825 (including Wilhelm Weber, well known to physicists in connection with electromagnetism), clearly shows the special nature of the ellipse. This experiment almost perfectly anticipates the Eigler group's measurements of matter waves 175 years later, since the image corresponds to drops of mercury landing at one focus with the other focus "empty."

Our theory of the quantum mirage (Fiete *et al.*, 2001) is based on a fairly straightforward modification of the scattering theory originally presented by Heller *et al.* (1994) (for non-Kondo atoms) to account for the Kondo effect. As we emphasized at the end of Sec. VII.A, for experimental temperatures below T_K we are able to take advantage of Nozieres's (1974) "local Fermi-liquid"
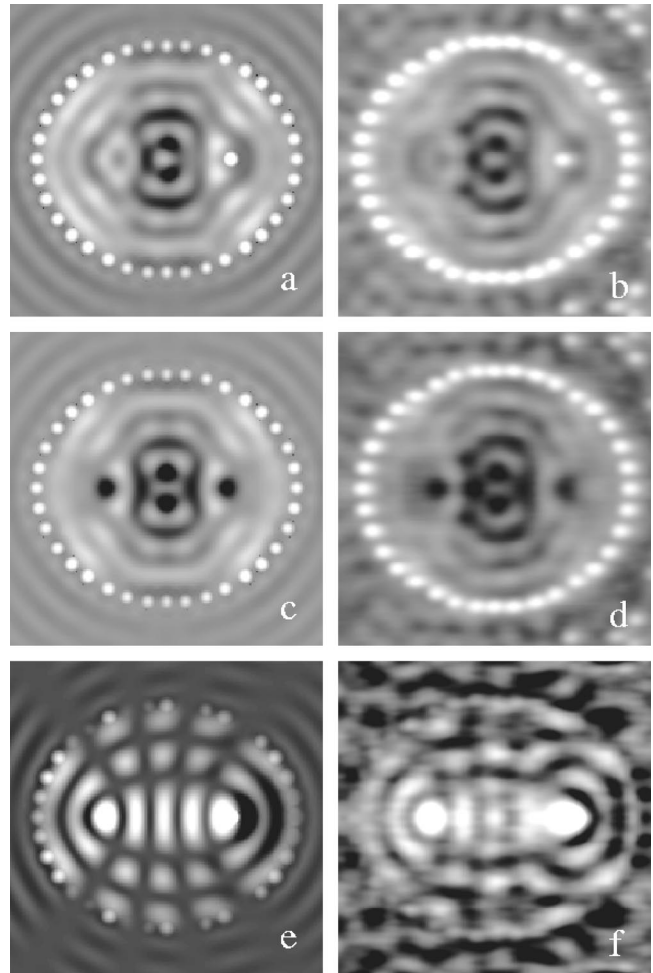
FIG. 12. dI/dV standing-wave patterns of a Kondo corral using the same theoretical vs experimental arrangement as in Fig. 11. dI/dV measurements were taken simultaneously with topographic images at a 10-meV bias. Note that (e) and (f) resemble an eigenstate of the ellipse. The ellipse was constructed to have large surface-state amplitudes at the two foci.

picture to write down a phenomenological single-particle theory with an energy-dependent phase shift. Our theory of the quantum mirage involves the following approximations, assumptions, and limitations: (i) The scattering of electrons from the adatoms is determined by a single parameter, the *s*-wave phase shift, and this must be determined from experiment or otherwise. (ii) The internal degrees of freedom (spin) of the Kondo adatoms are "frozen out" at the temperature of the experiment (~ 4 K) so we may use the results of Nozieres (1974) to treat the Kondo atom as a potential scatterer with a phase shift. (iii) The adatoms are far enough apart so that we may treat the electron propagation between them as free and that Ruderman-Kittel-Kasuya-Yosida (RKKY) interactions are sufficiently weak that the single-impurity Kondo physics is not altered. (iv) The theory does not include any nonequilibrium effects and does not treat the charge density within 7 Å of an atom correctly.

To make a direct comparison with experiment, we must obtain the phase shift of the Kondo adatoms. We

do not have an *ab initio* calculation of the phase shift of a single Co adatom. Rather, we fit the resonant form of the phase shift, including inelasticity due to the coupling of the surface states to bulk states, and calculated the multiple-scattering problem with this single atom data.

Since the on-atom electron orbital density is not accounted for in scattering theory, we used an on-atom fit [from experimental data of a single, isolated Co atom on Cu(111) at 4 K] involving only a renormalization of the free-space Green's function, $G_0^{\text{ret}}(\mathbf{r}', \mathbf{r}, \epsilon)$, and a change in the background phase shift to compute the STM signal on top of a Kondo adatom (Kawasaka *et al.*, 1999; Schiller and Hershfield, 2000; Plihal and Gadzuk, 2001; Shimada *et al.*, 2003). This on-atom fit is not part of our theory, but only a means of setting a reference point between on-atom density not accounted for in our theory and the electron density anywhere more than 7 Å away from an atom on the surface (which *is* accounted for properly in our theory). This fit in no way compromises our fundamental result that the mirage is due to resonantly scattering electrons from the Kondo atoms of the walls and focus. It is used only as a method for determining as accurately as possible the phase shift of the Co on Cu(111). Determining the phase shift this way from experimental data constitutes a measurement of the single Kondo atom phase shift. We find a good fit to the *s*-wave phase shift to be given by

$$\delta(\epsilon) = \delta_{bg} + i\,\delta'' + \tan^{-1}\!\left(\frac{\epsilon - \epsilon_0}{\Gamma/2}\right), \qquad (27)$$

where $\delta_{bg} = (\pi/4) \pm (\pi/10)$, $\delta'' = 3/2 \pm 1/4$, $\Gamma = (9 \pm 1)$ MeV, and $\epsilon_0 = E_F - 1$ meV are determined by experiment; δ_{bg} is a background phase shift (possibly due to static charge screening at the impurity) that controls the resonant line shape of the adatom scattering cross section;[20] and δ'' is a measure of the inelasticity in adatom scattering and controls the attenuation of the mirage at the empty focus. $\tan^{-1}[(\epsilon - \epsilon_0)/(\Gamma/2)]$ reflects resonant scattering due to the presence of Kondo physics and can be seen to follow directly from Eq. (22) and the density of states shown in Fig. 9. A similar phase shift (without the inelastic piece, δ'') would result from the model of Újsághy *et al.* (2000). It is likely that both bulk and surface states are participating in the Kondo effect at an adatom,[21] but the STM signal is more sensitive to the surface-state Kondo effect in the regime of validity of our theory (>7 Å away from an adatom).

Applying the scattering theory of Sec. IV and the phase shift, Eq. (27), to elliptical corrals results in the images shown in Figs. 11 and 12. The agreement with experiment is excellent. Our calculation of the tunneling spectrum at the two foci is compared with experiment in
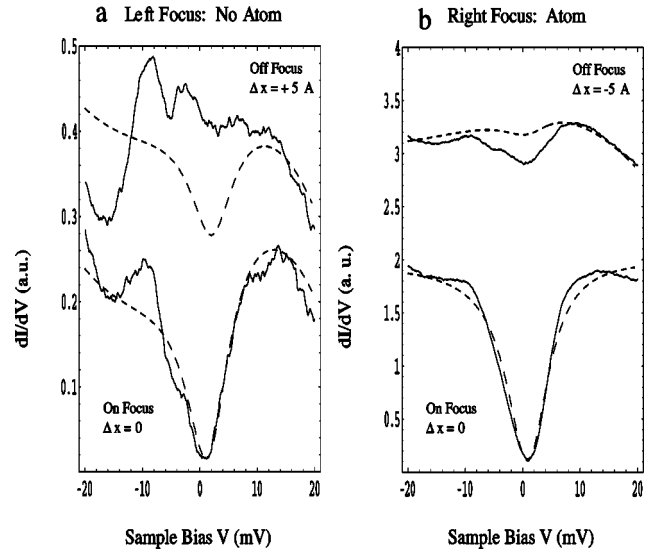

FIG. 13. Tunneling into the focal atom and empty focus: the mirage. Tunneling spectroscopy is calculated (dashed lines) with the scattering theory and phase shift given in the text at the empty focus (a). Tunneling spectroscopy at the occupied focus is shown in (b). A constant background slope has been removed from both the experimental data and the calculation. The attenuation of the mirage is determined by inelasticity in the scattering of electrons at the walls of the ellipse. The theoretical signal 5 Å away from the empty focus in (a) is lost in the noise of the experiment and is not a breakdown of the theory.

Fig. 13. Note that the signal at the unoccupied focus is attenuated by approximately a factor of 8, both experimentally and theoretically. The calculated spectroscopy in Fig. 13 most clearly demonstrates that the Kondo mirage is due only to resonant scattering of electrons from the Co adatom at the opposite focus, even though the electrons are also resonantly scattering from the wall adatoms: Calculations performed with $\delta = i\infty$ (Heller *et al.*, 1994) instead of $\delta(\epsilon)$ from Eq. (27) for the wall atoms show the Kondo resonances of the wall atoms play no essential role in the projection of the mirage to the empty focus since the signal in Fig. 13 is essentially unchanged. Experimentally the same result is found when the wall Co adatoms are replaced by CO (Manoharan *et al.*, 2000).

Only certain ellipses will give a good mirage effect—those which have large surface-state amplitudes at the foci when the scattering problem is calculated—and this depends on the relative dimensions of the ellipse and on λ_F. Only then will there be appreciable surface-state electron amplitude at the focal adatom to give a strong signal of Kondo effect in the surface states of Cu(111) at the opposite focus.[22] Our theory predicts that the quan-

tum mirage is not restricted to an ellipse or even a "closed" structure. Anytime one can construct an arrangement of adatoms or other defects that lead to a buildup of surface-state electron amplitude at two locations within the coherence length of the electron, a mirage can be projected.

In conclusion, the quantum mirage reveals no information about local polarization of the surface-state (or bulk) electrons. The unpolarized STM cannot measure the size of the Kondo "screening cloud" since it only returns an average signal of spin-up and spin-down electrons (or holes) tunneling into the surface. However, there are still several important things that can be learned from a combination of scattering theory and experiment about Kondo impurities on the surfaces of noble metals. First, Kondo impurities still act, to a large extent, like "black dot" scatterers. This is clear from the appreciable imaginary part of the scattering phase shift given in Eq. (27). The Kondo effect does not "block" or inhibit the scattering of surface-state electrons into the bulk at the impurities.[23] Second, the Fano line shape of the quantum mirage can be understood from a resonance in the scattering phase shift with a nonzero background phase shift. This complements the "on-atom" picture of the Fano resonance in dI/dV which can be thought of as electrons tunneling into both the conduction-electron states of the host (of surface and bulk character) and electrons tunneling into the "d level" of the impurity (Li, Schneider, Berndt, and Delley, 1998b; Madhavan *et al.*, 1998; Schiller and Hershfield, 2000; Plihal and Gadzuk, 2001). For an STM tip initially above a Kondo impurity, one can think of the Fano line shape from tunneling as "rolling over" to a Fano line shape from scattering when the tip moves laterally away from an impurity (Újsághy *et al.*, 2000; Fiete *et al.*, 2001). Third, the fact that the atoms in corral walls show a Kondo resonance much the same as the resonance from an isolated impurity on the surface means that the RKKY interaction between impurities is very weak. Moreover, the mirage is independent (both theoretically and experimentally) of the character of the wall atoms. In the corrals that show a strong mirage the surface-state electron density is small near the walls, yet the STM signal of the wall atoms is more or less unchanged. This suggests that it is mostly the bulk electrons that are involved in the Kondo effect. This is the same conclusion that has been reached recently by Knorr *et al.* (2002) from studies of a single Kondo impurity.

IX. RELATED WORK AND RECENT DEVELOPMENTS

Recently there have been several important developments in the study of quantum corrals, especially related to the recent mirage experiments and studies of the lifetimes of quasiparticles in the surface states. While our scattering theory explains nearly all of the observed features of quantum corrals, including the mirage experiments, it is phenomenological and based on a single-particle model. A full understanding of the surface-state response to magnetic impurities requires more detailed studies: experimentally with spin-resolved STM and theoretically with first-principles and many-body calculations. It is necessary to go beyond the single-particle theory, for example, to accurately calculate quantities such as spin-spin correlation functions of impurities in quantum corrals, details of the Kondo effect itself, or the way in which surface-state lifetimes can be modified by quantum corrals. Some of these studies have already been undertaken and we briefly describe them below.

A. Experiments

Since the mirage experiments, there have been few experimental studies specific to corrals reported; however, Kliewer, Berndt, and Crampin (2000) have studied the effect of the modification of surface-state electron density by corrals on the spectroscopy of Mn on Ag(111) and Kliewer *et al.* (2001) and Braun and Rieder (2002) have used quantum corrals and related structures to obtain information about the many-body lifetime effects in the surface states. Most STM studies have focused on the Kondo effect from the impurities themselves. Chen *et al.* (1999) reported the disappearance of the Kondo resonance for Co dimers on Au(111). Jamneala *et al.* (2000) carried out a systematic study of elements with atomic 3-d orbitals on Au(111). Odom *et al.* (2000) reported Kondo effect from Co *clusters* adsorbed on single wall metallic nanotubes.[24] Madhavan *et al.* (2001) studied Co on Au(111) as a function of impurity coverage from isolated impurities up to one monolayer. Nagoaka *et al.* (2002) looked at the temperature dependence of the broadening of the Kondo resonance of Ti on Ag(100). Schneider *et al.* (2002) measured the scattering phase shift from isolated Co atoms on Ag(111) and Knorr *et al.* (2002) studied the role of surface and bulk state contributions to the Kondo effect for Co on Cu(100) and Cu(111).

B. Theory

On the theoretical side, much more work has focused on the quantum mirage in corrals rather than on the single impurities. Agam and Schiller (2001), Porras *et al.* (2001), and Weissmann and Bonadeo (2001) have also developed theories for the quantum mirage based on a single-particle picture. More recently, Aligia (2001) and Shimada *et al.* (2002) developed a many-body theory of the quantum mirage. Chiappe and Aligia (2002) and

---

[23]In principle, the Kondo effect should lessen the incoherent scattering at the atoms because it tends to "freeze out" the spin, when compared to Fe impurities, for example. (This assumes, of course, that spin-flip scattering is indeed important at the Fe impurities.)

---

[24]The Kondo effect generated by a ferromagnetic cluster turns out to have several interesting and nontrivial new features compared to a single impurity (Fiete *et al.*, 2002).

Correa *et al.* (2002) have undertaken studies of the interaction between two magnetic impurities in a quantum corral. A model of interactions between two impurities in states confined to the surface of a sphere was studied by Hallberg *et al.* (2002). A recent renormalization-group study carried out by Cornaglia and Balseiro (2002) for Kondo impurities in nanoscale systems also makes contact with the mirage experiments. A recent work by Morr and Stavropoulos (2003) looks at the quantum mirage from non-Kondo impurities in a quantum corral built on a superconductor.

While there are now several theories addressing the physics of the mirage, we feel the least addressed question is that of the relative role of surface and bulk states in the formation of the Kondo effect at a single impurity. Many theories tend to neglect the bulk states and treat the quantum corral as a confined two-dimensional system. We believe theory should now move beyond this and include the role of both surface states and bulk states in Kondo resonance. It remains clear, however, that the mirage effect is dominated by a Kondo effect that *involves* the surface-state electrons because the phase shift, Eq. (27), demands it.

X. VARIATIONS OF "QUANTUM" CORRALS: OPTICAL CORRALS AND ACOUSTICAL CORRALS

Recently there have been several interesting variations of "quantum" corrals. Most notably, there are now both theory (de Francs *et al.*, 2001; Wubs and Lagendijk, 2002) and experimental realizations (Chicanne *et al.*, 2002) of optical quantum corrals and related structures. The theory of optical corrals is quite similar to quantum corrals, the main difference being that the electric field is a vector field while the wave function is a scalar field. In the optical corrals the adatoms are replaced by "posts" of a different dielectric constant to confine the electric field.

The same basic physics of quantum corrals also applies to acoustical corrals in which one can define a LDOS of states that is a local acoustical impedance function. The impedance is of course determined by the same "in-phase" vs "out-of-phase" condition of the returning wave relative to the outgoing wave. A map of acoustical impedance as a function of position in the room should show exactly the same type of oscillation with distance as does the STM dI/dV data. This serves to again remind us that the STM images are not "snapshots" of a wave caught in a cavity, such as water waves in a bathtub at some moment. In fact the analogy of the quantum corrals and room acoustics is quite close, since a Q factor of 2 is not unusual for relatively "quiet" rooms.

XI. CONCLUSIONS

In this Colloquium we have reviewed the basic physics of quantum corrals, including the more recent experiments involving the Kondo effect. A single-particle scattering theory with only an s-wave phase shift is able to account quantitatively for nearly all of the experimental observations to date, including the quantum mirage. It is a generic feature of adatoms on the surfaces of the noble metals that they strongly couple the surface states to the bulk states. This appears in the scattering theory as an imaginary part of the phase shift. When the adatoms are magnetic and below their Kondo temperature, the many-body Kondo resonance can be taken into account phenomenologically with a resonance in the phase shift, Eq. (27).

The scattering theory that we have presented is valid anywhere more than ~ 7 Å away from an adatom since this is the scale over which an adatom strongly disturbs the local charge density. From Kondo impurities there is Fano resonance in dI/dV that persists as the STM tip is moved from directly over a Kondo atom to a location where it is 10 Å or more laterally away. For Kondo impurities, the ~ 10-Å spatial extent of the Fano line shape in dI/dV is *not a measure of the Kondo screening cloud*. To date all reported STM studies of Kondo impurities have been unpolarized and hence they are insensitive to local spin polarization. What the ~ 10-Å spatial scale most likely reflects is the scale over which the STM tip can strongly couple to the atomic states of the impurities. Hence, it is a scale associated with charge rather than spin. The mirage, therefore, reflects nothing about local spin correlations at the empty focus of the elliptical quantum corral. It is simply a way of probing the Kondo resonance of the impurity at the opposite focus through coherent electron propagation in the surface states. The signal at the empty focus can be thought of as a "scattering" Fano resonance originating from a resonance piece and an energy-independent background piece in the scattering phase shift of the Kondo atom.

The new frontiers in quantum corral experiments clearly lie in two directions: (i) spin-polarized STM and (ii) probes of many-body physics. There are already several theories that predict strong spin correlations between impurities in corrals (Chiappe and Aligia, 2002; Correa *et al.*, 2002; Gyorffy, 2002) although none have yet been experimentally reported. The relative role of bulk and surface states in the Kondo effect is still an open question, although experimental progress has been made (Knorr *et al.*, 2002) which suggests that the Kondo effect is dominated by bulk states. Quantum corrals can also provide tunable environments to study and even modify the physics of the surface states themselves (Kliewer *et al.*, 2001; Braun and Rieder, 2002). With ever improving experimental technology we expect to see even more surprises and fascinating effects to appear in these tiny, engineered laboratories of many-body physics.

ACKNOWLEDGMENTS

REFERENCES

Agam, O., and A. Schiller, 2001, Phys. Rev. Lett. **86**, 484.

Aligia, A. A., 2001, Phys. Rev. B **64**, 121102(R).

Anderson, P. W., 1961, Phys. Rev. **124**, 41.

Anderson, P. W., 1970, J. Phys. C **3**, 2439.

Bracher, C., M. Riza, and M. Klever, 1997, Phys. Rev. B **56**, 7704.

Braun, K.-F., and K.-H. Rieder, 2002, Phys. Rev. Lett. **88**, 096801.

Bürgi, L., O. Jeandupeux, H. Brune, and K. Kern, 1999, Phys. Rev. Lett. **82**, 4516.

Bürgi, L., O. Jeandupeux, A. Hirstein, H. Brune, and K. Kern, 1998, Phys. Rev. Lett. **81**, 5370.

Chan, S., 1997, Ph.D. thesis (Harvard University).

Chen, C. J., 1993, *Introduction to Scanning Tunneling Microscopy* (Oxford, New York).

Chen, W., T. Jamneala, V. Madhavan, and M. F. Crommie, 1999, Phys. Rev. B **60**, R8529.

Chiappe, G., and A. A. Aligia, 2002, Phys. Rev. B **66**, 075421.

Chicanne, C., T. David, R. Quidant, J. C. Weeber, Y. Lacroute, E. Bourillot, A. Dereux, G. C. des Francs, and C. Girard, 2002, Phys. Rev. Lett. **88**, 097402.

Cornaglia, P. S., and C. A. Balseiro, 2002, Phys. Rev. B **66**, 115303.

Correa, A., K. Hallberg, and C. A. Balseiro, 2002, Europhys. Lett. **58**, 899.

Crampin, S., M. H. Boon, and J. I. Inglesfield, 1994, Phys. Rev. Lett. **73**, 1015.

Crampin, S., and O. R. Bryant, 1996, Phys. Rev. B **54**, R17 367.

Crommie, M. F., C. P. Lutz, and D. M. Eigler, 1993a, Science **262**, 218.

Crommie, M. F., C. P. Lutz, and D. M. Eigler, 1993b, Nature (London) **363**, 524.

Crommie, M. F., C. P. Lutz, D. M. Eigler, and E. J. Heller, 1995, Physica D **83**, 98.

Crommie, M. F., C. P. Lutz, D. M. Eigler, and E. J. Heller, 1996, Surf. Sci. **361-362**, 864.

Davison, S. G., and M. Steslicka, 1996, *Basic Theory of Surface States* (Oxford, New York).

de Francs, G. C., C. Girard, J.-C. Weeber, C. Chicane, T. David, A. Dereux, and D. Peyrade, 2001, Phys. Rev. Lett. **86**, 4950.

Eigler, D. M., and E. K. Schweizer, 1990, Nature (London) **344**, 524.

Fiete, G. A., J. S. Hersch, E. J. Heller, H. C. Manoharan, C. P. Lutz, and D. M. Eigler, 2001, Phys. Rev. Lett. **86**, 2392.

Fiete, G. A., G. Zaránd, B. I. Halperin, and Y. Oreg, 2002, Phys. Rev. B **66**, 024431.

Gyorffy, B., 2002, private communication.

Hallberg, K., A. A. Correa, and C. A. Balseiro, 2002, Phys. Rev. Lett. **88**, 066802.

Harbury, H. K., and W. Porod, 1996, Phys. Rev. B **53**, 15 455.

Hasegawa, Y., and P. Avouris, 1993, Phys. Rev. Lett. **71**, 1071.

Heller, E. J., 1984, Phys. Rev. Lett. **53**, 1515.

Heller, E. J., M. F. Crommie, C. P. Lutz, and D. Eigler, 1994, Nature (London) **369**, 464.

Heller, E. J., M. F. Crommie, C. P. Lutz, and D. Eigler, 1995, in *The Physics of Electronic and Atomic Collisions*, edited by L.

J. Dubé, J. B. A. Mitchell, J. W. McConkey, and C. E. Brion, AIP Conf. Proc. No. 360 (AIP, Woodbury, NY).

Hewson, A. C., 1997, *The Kondo Problem to Heavy Fermions* (Cambridge University, Cambridge, England).

Hormandinger, G., and J. B. Pendry, 1994, Phys. Rev. B **50**, 18 607.

Jamneala, T., V. Madhavan, W. Chen, and M. F. Crommie, 2000, Phys. Rev. B **61**, 9990.

Jeandupeux, O., L. Bürgi, A. Hirstein, H. Brune, and K. Kern, 1999, Phys. Rev. B **59**, 15 926.

Kawasaka, T., H. Kasai, W. A. Diño, and A. Okiji, 1999, J. Appl. Phys. **86**, 6970.

Kevan, S. D., and R. H. Gaylord, 1987, Phys. Rev. B **36**, 5809.

Kliewer, J., R. Berndt, E. V. Chulkov, V. M. Silkin, P. M. Echenique, and S. Crampin, 2000, Science **288**, 1899.

Kliewer, J., R. Berndt, and S. Crampin, 2000, Phys. Rev. Lett. **85**, 4936.

Kliewer, J., R. Berndt, and S. Crampin, 2001, New J. Phys. **2**, 22.

Knorr, N., M. A. Schneider, L. Diekhöner, P. Wahl, and K. Kern, 2002, Phys. Rev. Lett. **88**, 096804.

Kondo, J., 1964, Prog. Theor. Phys. **32**, 37.

Li, J., W.-D. Schneider, R. Berndt, O. R. Bryant, and S. Crampin, 1998a, Phys. Rev. Lett. **81**, 4464.

Li, J., W.-D. Schneider, R. Berndt, and B. Delley, 1998b, Phys. Rev. Lett. **80**, 2893.

Madhavan, V., W. Chen, T. Jamneala, and M. F. Crommie, 2001, Phys. Rev. B **64**, 165412.

Madhavan, V., W. Chen, T. Jamneala, M. F. Crommie, and N. S. Wingreen, 1998, Science **280**, 567.

Manoharan, H. C., C. P. Lutz, and D. M. Eigler, 2000, Nature (London) **403**, 512.

Morgenstern, K., K.-F. Braun, and K.-H. Rieder, 2002, Phys. Rev. Lett. **89**, 226801.

Morr, D. K., and N. A. Stavropoulos, 2003, e-print cond-mat/0304533; http://xxx.lanl.gov/abs

Nagoaka, K., T. Jamneala, M. Grobis, and M. F. Crommie, 2002, Phys. Rev. Lett. **88**, 077205.

Nozieres, P., 1974, J. Low Temp. Phys. **17**, 31.

Nozieres, P., and A. Blandin, 1980, J. Phys. (France) **41**, 193.

Odom, T. W., J.-L. Huang, C. L. Cheung, and C. M. Lieber, 2000, Science **290**, 1549.

Plihal, M., and J. W. Gadzuk, 2001, Phys. Rev. B **63**, 085404.

Porras, D., J. Fernández-Rossier, and C. Tejedor, 2001, Phys. Rev. B **63**, 155406.

Rodberg, L. S., and R. M. Thaler, 1967, *Introduction to the Quantum Theory of Scattering* (Academic, New York).

Schiller, A., and S. Hershfield, 2000, Phys. Rev. B **61**, 9036.

Schneider, M. A., L. Vitali, N. Knorr, and K. Kern, 2002, Phys. Rev. B **65**, 121406(R).

Schrieffer, J. R., and P. A. Wolf, 1966, Phys. Rev. **149**, 491.

Shimada, Y., H. Kasai, H. Nakanishi, W. A. Dino, A. Okiji, and Y. Hasegawa, 2002, Surf. Sci. **89**, 514.

Shimada, Y., H. Kasai, H. Nakanishi, W. A. Diño, A. Okiji, and Y. Hasegawa, 2003, J. Appl. Phys. **94**, 334.

Tersoff, J., and D. R. Hamann, 1985, Phys. Rev. B **31**, 805.

Újsághy, O., J. Kroha, L. Szunyogh, and A. Zawadowski, 2000, Phys. Rev. Lett. **85**, 2557.

Újsághy, O., G. Zaránd, and A. Zawadowski, 2001, Solid State Commun. **117**, 167.

Weissmann, M., and H. Bonadeo, 2001, Physica E (Amsterdam) **10**, 44.

Wubs, M., and A. Lagendijk, 2002, Phys. Rev. E **65**, 046612.